NUREG/CR–6074
04–0448–010
Vol. 5

Sealed Source and Device Design Safety Testing

Technical Report on the Findings of Task 4

Investigation of Failed Radioactive Stainless Steel Troxler Gauges

Manuscript Completed: October 1995
Date Published: October 1995

Prepared by
D. J. Benac, W. R. Schick

Southwest Research Institute
6220 Culebra Road
San Antonio, TX 78238–5166

D. H. Tiktinsky, NRC Project Manager

Prepared for
Division of Industrial and Medical Nuclear Safety
Office of Nuclear Material Safety and Safeguards
U.S. Nuclear Regulatory Commission
Washington, DC 20555–0001
NRC Job Code D2553

DISCLAIMER

Abstract

This report covers the Task 4 activities for the Sealed Source and Device Safety testing program. SwRI was contracted to investigate failed radioactive stainless steel troxler gauges. SwRI's task was to determine the cause of failure of the rods and the extent of the problem. SwRI concluded that the broken rod failed in a brittle manner due to a hard zone in the heat affected zone.

Table of Contents

List of Figures

List of Figures (continued)

List of Tables

Acknowledgements

The authors would like to acknowledge the following Southwest Research Institute staff for their contribution in this failure investigation. Special mention goes to the Southwest Research Institute Radiation safety staff including Mr. Frank Iddings, Mr. Ty Schraeder, and Mr. John Hageman for their guidance on handling radioactive material.

Special recognition is warranted to the Southwest Research Institute Failure Analysis Laboratory staff including Mr. Ramsey Railsback, Mr. Isaac Rodriguez, and Mr. Harold Saldana.

Ms. Rachel Munoz is acknowledged for the clerical support.

Sealed Source and Device Safety Testing

Technical Report on the Findings of Task 4

Executive Summary

On August 8, 1993, the Ohio Department of Transportation reported that during routine use of a Troxler Model 3401 nuclear gauging device, the cesium 137 radioactive tip fell off. The gauge is used to measure density of asphalts, soils or other mediums. It was determined by the Ohio Department of Transportation that the break occurred in the vicinity of the weld that secured the encapsulated source to the probe. Southwest Research Institute was furnished the broken rod and four other rods to determine the cause for failure and the extent of the problem.

Southwest Research Institute concluded that the broken rod failed in a brittle manner due to a hard zone in the heat affected zone of the weld. Because the rod material, Type 440C, has poor weldability, it developed a hard zone that was not relieved with a post weld heat treatment. The fractographic evidence and surface abrasion marks indicated that the rod was subjected to a bending condition at the hardened zone which initiated a crack. After the crack had initiated, it gradually propagated during multiple uses.

The other rods evaluated appeared to be of a similar material based on hardness. However, the alloy of the rods were not confirmed because the radioactive rods were not allowed to be analyzed. One of the gauges was cracked in the same location and in a similar manner. This suggests that this type of brittle failure may occur in other rods. It does appear that the crack extension is progressive and should be identifiable visually or with penetrant inspection.

1.0 Introduction

The Ohio Department of Transportation (ODOT) reported on August 8, 1993 during a routine use of a Troxler Model 3401 nuclear gauging device that the radioactive tip fell off. The tip of the source tube contained 8 millicuries of cesium 137. The Troxler gauge, shown in Figure 1-1, is used to measure the density of asphalt, soils, and other mediums. The radioactive rod is inserted into a drilled hole in the asphalt, then the radiation at the gauge is measured. For density, the cesium 137 emits gamma radiation which enters the test medium. The denser the test material is, the more radiation is absorbed, thus, less radiation reaches the detector. Troxler Gauge No. 12711, shown in Figure 1-1, had the broken rod, shown in Figure 1-2. It was determined by ODOT that the break had occurred in the vicinity of the weld that secured the encapsulated source to the probe. Five gauges were submitted to Southwest Research Institute (SwRI) to determine the extent of the problem and mechanism of failure. Table 1-1 shows a list of the gauges and the status as identified by ODOT.

Table 2-1. Gauges Submitted to SwRI

Gauge No.	Condition (as reported by ODOT)
12711	Broken source rod
12706	Weld worn slightly
12712	Rod cracked
12710	Weld worn and possibly cracked
12717	OK- for standard comparison

SwRI investigated the broken source rod and evaluated the condition of the other rods. The specific tasks involved: (1) document the as-received condition of the gauges, (2) perform visual examination for extraneous damage, corrosion, or dents, (3) conduct dye penetrant inspection of the other rods, (4) determine the chemical composition of the rod, (5) determine the hardness level of the rods, (6) evaluate the weld condition and identify if the rod was properly welded, and (7) determine if all of the rods were constructed of the same alloy and in the same welded condition.

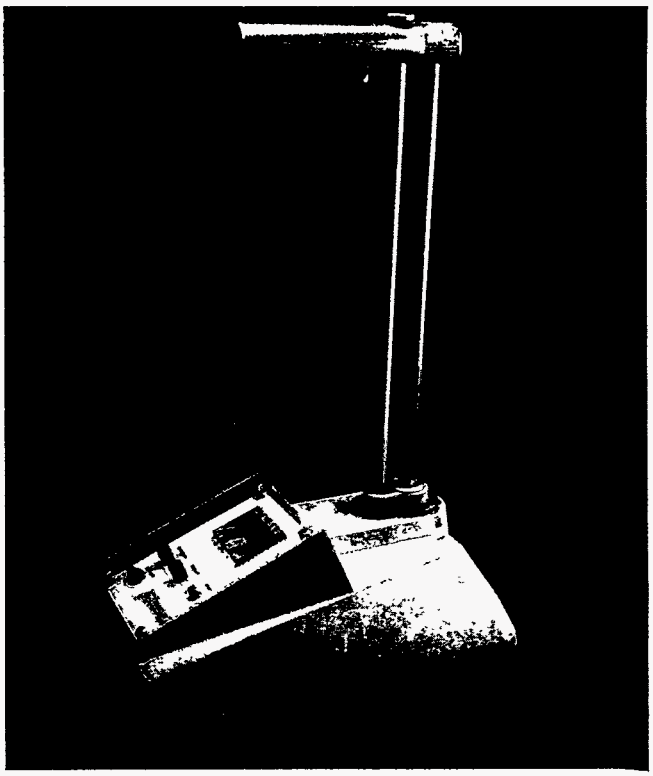

69481 ≈1/6X

a) Gauge No. 12711

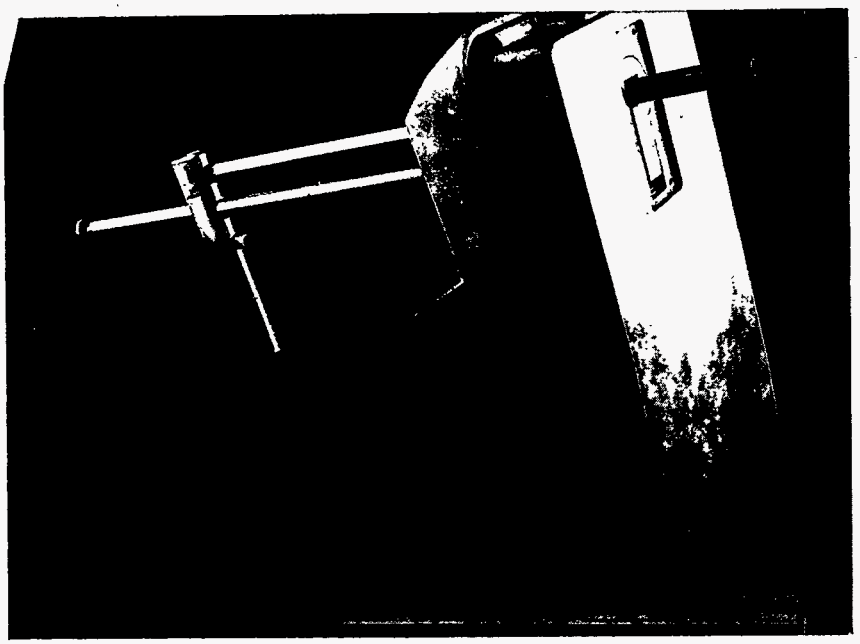

69482

b) Fractured Rod Extended

FIGURE 1-1. PHOTOGRAPHS OF THE AS-RECEIVED TROXLER GAUGE NO. 12711 (a) AND THE EXTENDED FRACTURED ROD (b).

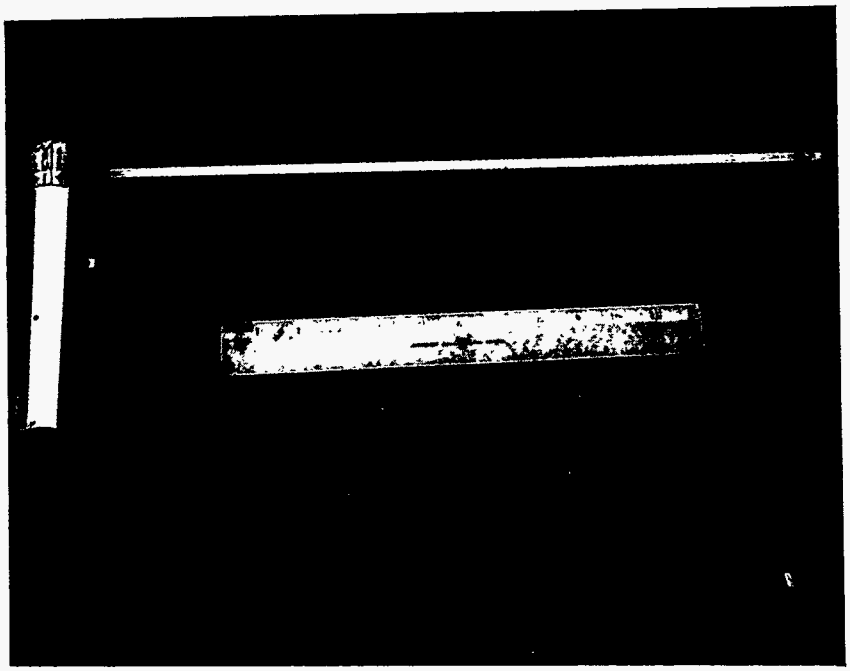

69492

a) Side View of Rod

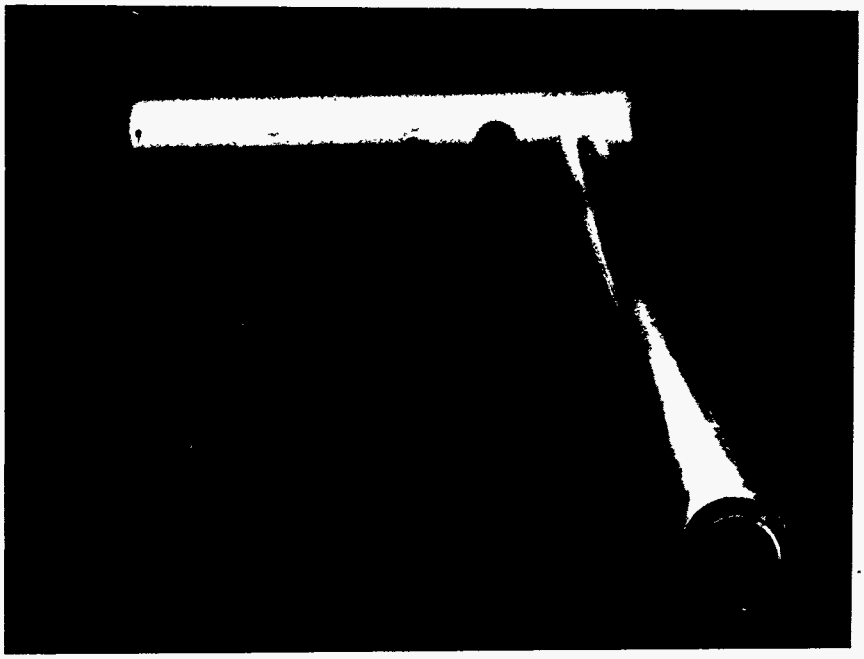

69493

b) End of Fractured Rod

FIGURE 1-2. PHOTOGRAPHS OF THE FAILED ROD.

2.0 Conclusions

(1) The Troxler Gauge No. 12711 failed in a brittle manner because of a hard zone that resulted from welding. The rod material, Type 440C, is a difficult alloy to weld. The combined effects of material selection, joint configuration, and welding procedure resulted in the hard zone.

(2) At some time during usage of the gauge in the field, the rod was impacted as indicated by abrasive markings. This caused a bending condition on the rod at the hard zone which resulted in a crack.

(3) Corrosion pits were present on the surface. Although the corrosion pit provided a preferred location to initiate a crack, the corrosion was not the cause for failure.

(4) After the crack initiated, the crack propagated progressively over multiple uses, eventually resulting in catastrophic failure after the crack had extended about 290° around the circumference. The cause for the progressive propagation was not exactly identified, but it is probable that the crack progressed due to bending cyclic load induced during usage.

(5) One of the Troxler gauges, No. 12712, received for evaluation had a crack that extended about 180° around the circumference. This further supports that the crack extension is progressive and not the result of one incident. The other gauges had no signs of cracking. Gauge No. 12710 that was suspected to be cracked was not.

(6) The rod and cup material were Type 440C, a hardenable chrome alloy. The rod and cup were welded using a Type 308 filler. Although this is a reasonable selection, Type 440C is difficult to weld and requires a pre- and post-weld heat treatment. It appears that the rods were not heat treated after welding.

(7) The exact alloy of construction for the other rods and cups were not determined because SwRI was not allowed to section the rods. However, the hardnesses were similar to the failed rod.

(8) SwRI believes that the failure of this rod may not be an isolated incident and that additional rods may crack, then fail. This conclusion is based on the fact that Gauge No. 12711 failed in a brittle manner and Gauge No. 12712 was cracked in the same position. Although the majority of the rods will not be cracked, if a rod is subjected to the same conditions as those evaluated in this investigation, then the rods are prone to cracking.

(9) Since the crack extension is progressive, a crack can be detected visually or by penetrant inspection if inspected in the field on a regular interval.

3.0 Macroscopic Evaluation

The macroscopic evaluation involved: (1) examining the OD surface of the rod for any signs of extraneous surface blemishes, (2) inspecting of the rods using dye penetrant, and (3) determining radiation levels.

The radiation levels were measured using a calibrated survey meter. The radiation levels are as reported in Table 3-1.

Table. 3-1. Radiation Levels for the Rods

Gauge No.	On Contact (mR/HR)	At 6 inches (mR/HR)
12706	360	30
12710	650	50
12712	1,000	40
12717	940	30

Due to the radiation levels of the four encapsulated sources, the surfaces were examined at low magnification from a distance. The surfaces looked similar to the failed rod surface. Documentation was conducted on the failed rod since it did not have high radiation levels. The surface of the failed rod had extensive scoring and signs of superficial rusting in isolated locations. Figure 3-1 shows the rust-like corrosion appeared to be random in nature, but, between about 1.0 to 1.5 inch from the end, no pitting was found. It was later confirmed that this region was the austenitic weld.

Three of the four gauges were red-dye penetrant inspected. Gauge No. 12712 had a crack present in a similar location as the failed rod. The crack extended nearly 180° around the circumference. Gauges No. 12706 and 12710 did not have any indication of a crack. Gauge No. 12710 had indications of smeared metal. The smeared metal was about 1.0 to 1.25 inches from the end. Although, Gauge No. 12710 had a suspected crack, it actually was burnished material that was smeared.

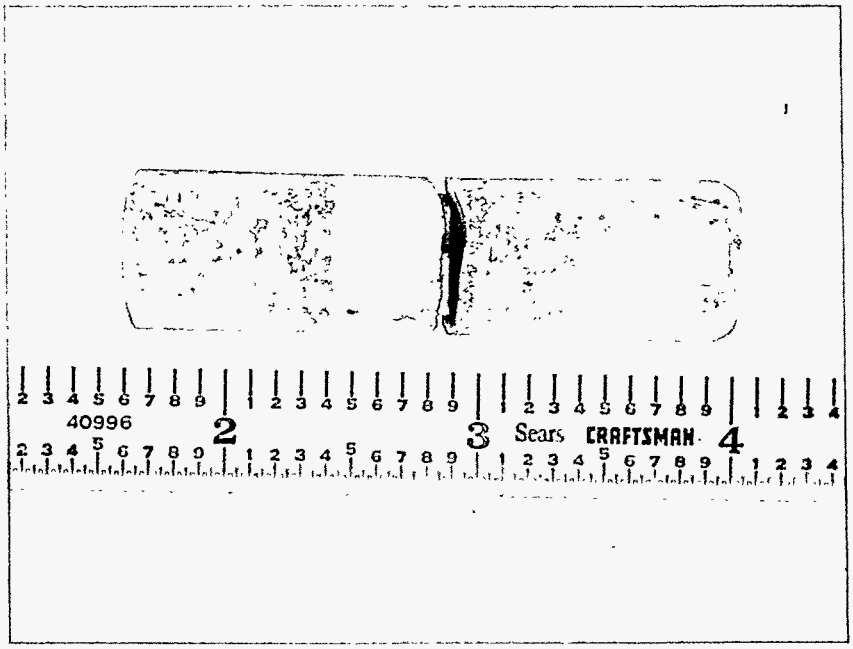

69528

a) Mating Fractures

69566 10X

b) As-Received Surface

FIGURE 3-1. PHOTOGRAPHS OF THE TIP AND LOCATION OF FAILURE.
Arrow shows abrasive mark on OD surface.

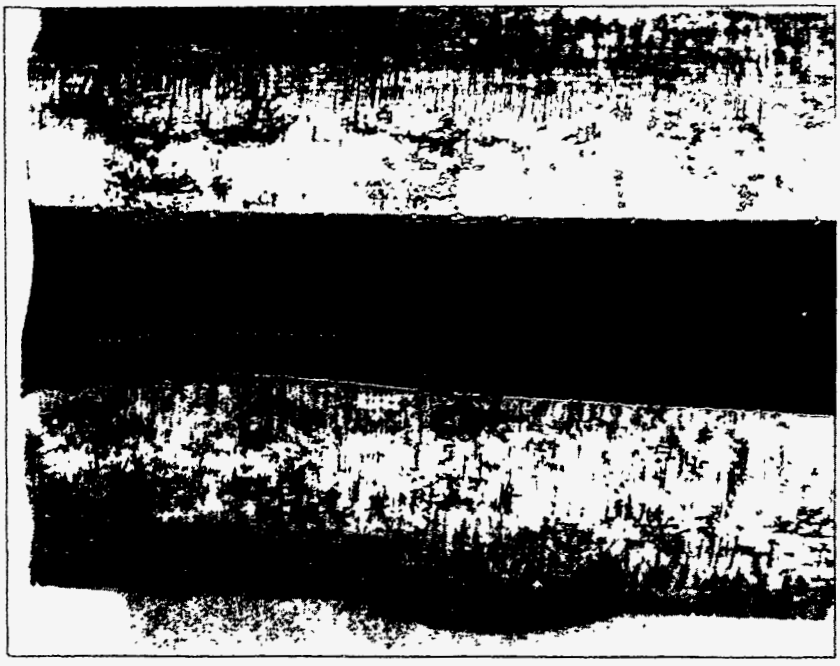

69566 10X

b) As-Received Surface

FIGURE 3-1 (continued). PHOTOGRAPHS OF THE TIP AND LOCATION OF FAILURE.

4.0 Material Evaluation

Chemical Analysis

Table 4-1 shows the chemical analysis results from the fractured rod, Gauge No. 12711. In order to determine the composition, a small slice was sectioned from the rod away from the fracture and towards the housing. The results indicated that the rod material was an AISI 440C, which is a hardenable chrome stainless steel. It was reported by Troxler personnel that some of the rods were made from 17-4PH stainless steel. The composition is shown for comparison purposes.

The ASTM test methods used to determine the chemical composition of the rod were E663, E1019, E354, and E1479.

Table 4-1. Chemical Composition of the Rod

Gauge No.	Composition (% by weight)								
	C	Mn	Si	Ni	Cr	Mo	P	S	Cu
No. 12711	1.08	0.46	0.33	0.22	17.2	0.28	0.012	0	-
AISI 440C	0.95-1.20	1.00 Max	0.33 Max	0.75 Max	16.0-18.0	0.75 Max	0.040 Max	0.030 Max	-
17-7PH	0.07 Max	1.00 Max	1.00 Max	3.0-5.0	15.0-17.0	-	0.040 Max	0.030 Max	3.0-5.0

Hardness Evaluation

Rockwell hardness (HRC) and diamond pyramid microhardness (DPH) tests were conducted on the rods received for evaluation. Because the radioactive level of the rods was as much as 1 mR/hr on contact, microhardness tests could not be conducted on four of the rods. For meaningful microhardness results, a flat area is desired. It was difficult to guarantee a flat area without increased radiation exposure to the technical staff. In addition, evaluation of the microhardness indent requires the technical staff to be directly over the radiation. For these reasons, microhardness tests were not conducted. In lieu of that, Rockwell HRC tests were performed using proper lead shielding. Because the rods were not flattened, the as-received surfaces were hardness tested.

Table 4-2 shows the hardness profile at various locations along the rods. One region, from 1.0 to 1.2 inch, on each of the rods had a very soft region (HRC 15.2 to 23.8). This region was the weld. The base metal away from the weld ranged from HRC values in the high 40s to mid 50s.

Table 4-3 shows the microhardness values for the failed Troxler Gauge No. 12711. The fracture plane was about 1.0 inches from the end of the rod. The fracture did not occur in the weld, but at the toe of the weld in the HAZ. Hardness measurements were made on either side of the fracture. The hardness results showed that at the location of crack initiation, the hardness was the highest. It was interesting to note that the weld was extremely soft. A weld usually is not as soft as shown in this rod. In fact, the hardness survey indicated that all of the rods had an extremely soft weld.

Table 4-2. Hardness Survey of Troxler Gauge Rods

	Hardness (HRC)			
Distance from End (inches)	**#12706**	**#12710**	**#12712**	**#12717**
1.6	-	-	-	48.2
1.5	-	56.5	50.1	33.0
1.4	-		-	43.2
1.2	45.7	15.2*	-	17.7*
1.1*	22.9*	23.8*	16.0*	25.4*
1.0	47.2	17.1	16.4	57.5
0.9	53.2	54.4	26.1	-
0.8	50.1	45.1	50.0	50.8
0.7	42.1	39.1	52.9	50.9
0.6	-	-	50.4	-
0.5	47.0	49.0	45.0	50.7

* These locations are hardness readings on the weld.

Table 4-3. Microhardness Results for the Failed Rod on Troxler Gauge No. 12711

Location	Microhardness (DPH)	Equivalent Hardness (HRC)	Position	Distance from Fracture Towards Housing
1	395.7	40.3	Base	0.394 mm.
2	367.9	37.5	Base	0.327 mm.
3	603.3	55.4	Base	0.287 mm.
4	438.1	44.3	HAZ	0.259 mm.
5	261.8	24.3	Weld	0.220 mm.
6	242.7	20.9	Weld	0.157 mm.
7	249.1	22.1	Weld	0.118 mm.
8	357.8	36.4	HAZ	0.079 mm.
9	325.1	32.7	HAZ	0.047 mm.
10	474.5	47.2	HAZ	0.016 mm.
11	707.5	60.4	At Fracture	n/a
Fracture				**Distance from Fracture Towards Rod End**
12	750.7	62.1	At Fracture	n/a
13	665.1	58.5	Base	0.016 mm.
14	572.7	53.7	Base	0.032 mm.
15	540.0	51.5	Base	0.055 mm.
16	413.0	42.0	Base	0.087 mm.
17	468.7	46.8	Base	0.122 mm.
18	582.9	54.3	Base	0.157 mm.
19	591.3	54.7	Base	0.197 mm.
20	606.3	55.6	Base	0.276 mm.
21	597.7	55.1	Base	0.331 mm.
22	599.8	55.2	Base	0.394 mm.

5.0 Metallographic Evaluation

Both halves of the fracture surface were sectioned in the vicinity of the origin to examine the weld and to determine if any microstructural anomaly caused the failure. Figure 5-1 shows the position of the weld relative to the fracture. Figure 5-2 shows a close-up of the weld heat affected zones (HAZ) and hardness indentations. The fracture plane was about 0.034 inch from the edge of the weld metal at the surface of the rod. The fracture origin location had no anomaly, however, the base metal was more typical of an untempered martensite, which is hard. The weld had a lack of fusion between the weld metal and the rod. But, this did not contribute to failure, see Section 8 - Weld Evaluation, for more details. Figure 5-3 shows the OD surface had corrosion pits. The corrosion pits were about 0.0025 inch deep. No cracks extended from the pits.

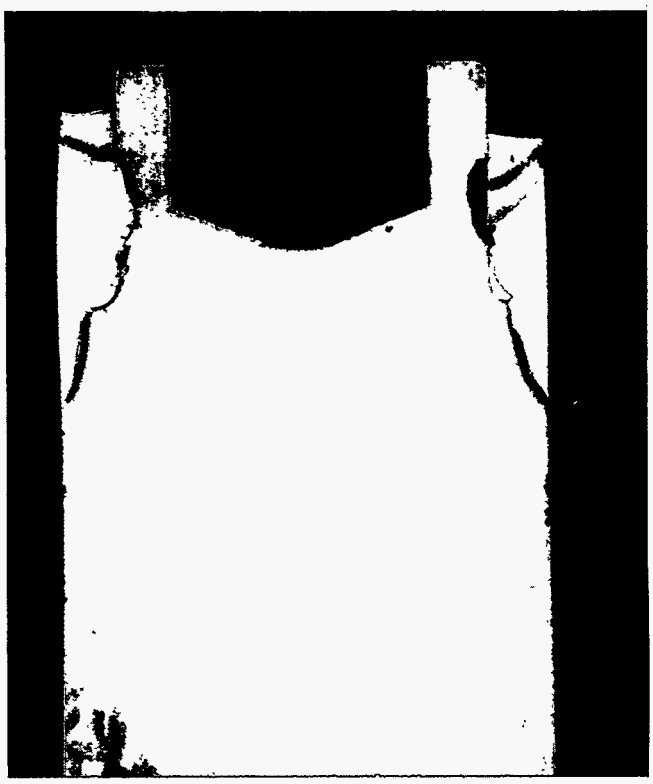

70004 4X

a)

70005 6X

b)

FIGURE 5-1. PHOTOMICROGRAPHS OF THE ROD CROSS SECTIONED AT THE FRACTURE.

FIGURE 5-2. PHOTOMICROGRAPHS OF THE ROD CROSS SECTIONED SHOWING THE WELD AND MICROHARDNESS LOCATIONS.

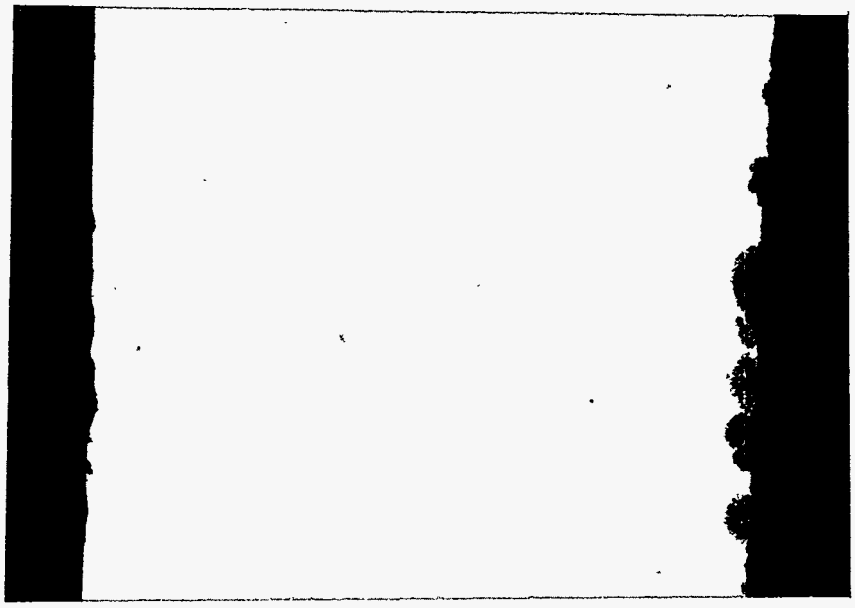

69740 50X

a)

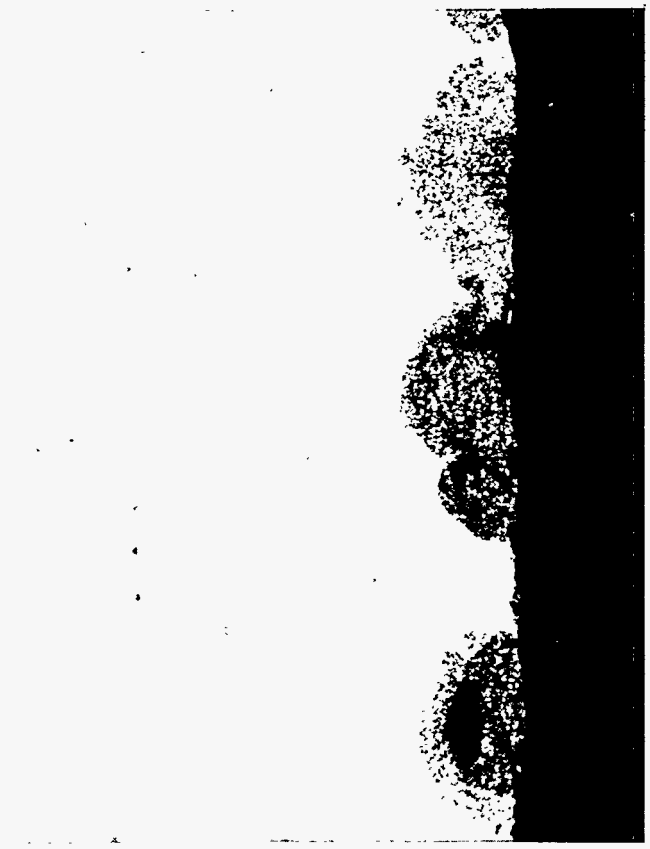

69741 200X

b)

FIGURE 5-3. PHOTOMICROGRAPHS OF THE OD SURFACE SHOWING CORROSION ATTACK. Notice no microcracks extend from the pits.

6.0 Fractographic Evaluation

The fracture surface from Gauge No. 12711 was examined using the stereomicroscope and the scanning electron microscope (SEM). Figure 6-1 shows the fracture surface viewed towards the end of the rod. Figure 6-2 shows the fracture surface viewed towards the housing. The fracture plane was nearly transverse to the axis of the rod. A unique feature found on the fracture surfaces was a discolored zone, shown in Figures 6-2 through 6-4. The discolored region extended about 0.25 inch around the circumference. The clamshell features and radial markings, shown in Figure 6-4, indicate this region was the origin. Crack initiation occurred on one side of the rod coinciding with the elliptical region. The transverse crack extension and the initiation on one side suggests that the rod was loaded in a bending condition.

To further understand the fracture mechanism and cause for initiation, various locations were examined on the fracture. The fracture was examined in the as-received condition and in the cleaned condition. SwRI cleaned the fracture using a hot alconox solution. The following items were observed.

1) The discolored region was elliptical in shape and had a heavy oxide present, see Figure 6-3.

2) Corrosion pits were evident in the vicinity of the origin, see Figures 6-4 and 6-5, however, pitting was not limited to the origin.

3) An abrasive-like scratch was evident in the vicinity of the origin, see Figure 6-6.

4) The fracture features in the elliptical region were flat. Although there were no obvious signs of fatigue striations, crack arrest bands were present indicative of progressive crack propagation. The crack extended about 290° before final fracture occurred.

5) There were no signs of tensile overload dimples, or cleavage facets in the origin location indicative of brittle impact overload, or even intergranular facets indicative of environmental attack, see Figures 6-5 and 6-7.

6) The fracture features in the final fracture region were primarily of brittle cleavage failure indicated by the facets (occasional dimples were also evident), see Figure 6-8.

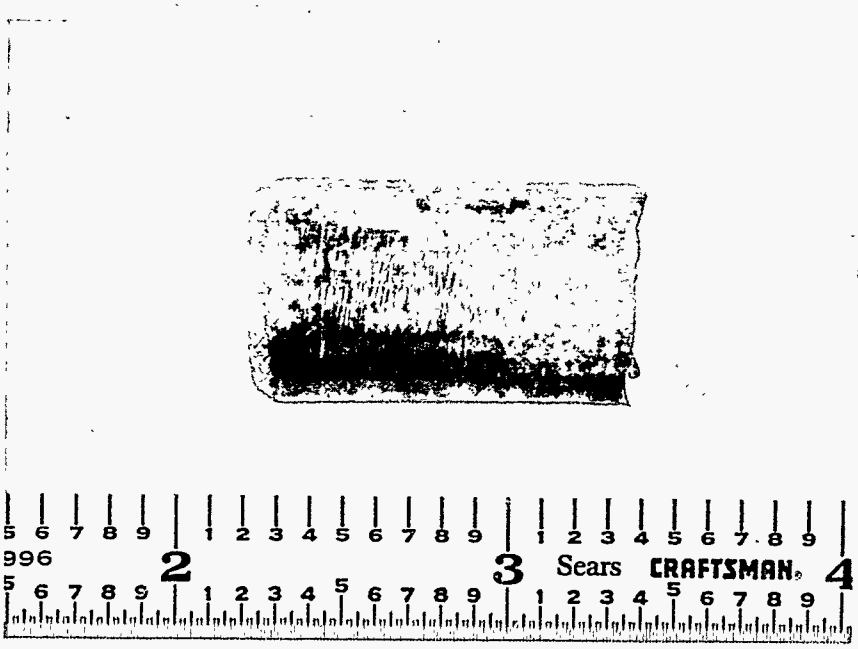

69392

a)

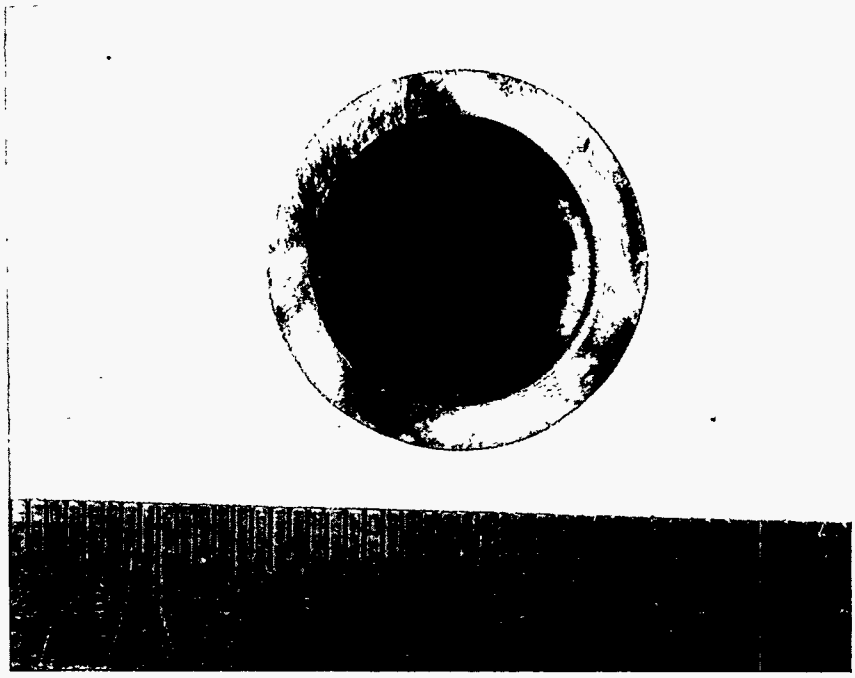

69393

b)

FIGURE 6-1. PHOTOGRAPHS OF THE FRACTURED TIP.

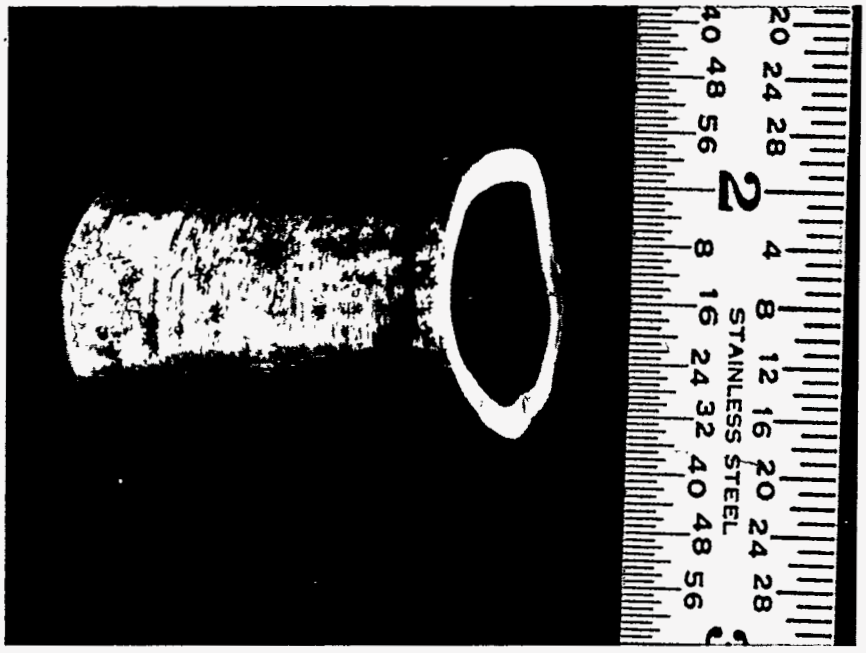

69394

c)

FIGURE 6-1 (continued). PHOTOGRAPHS OF THE FRACTURED TIP.

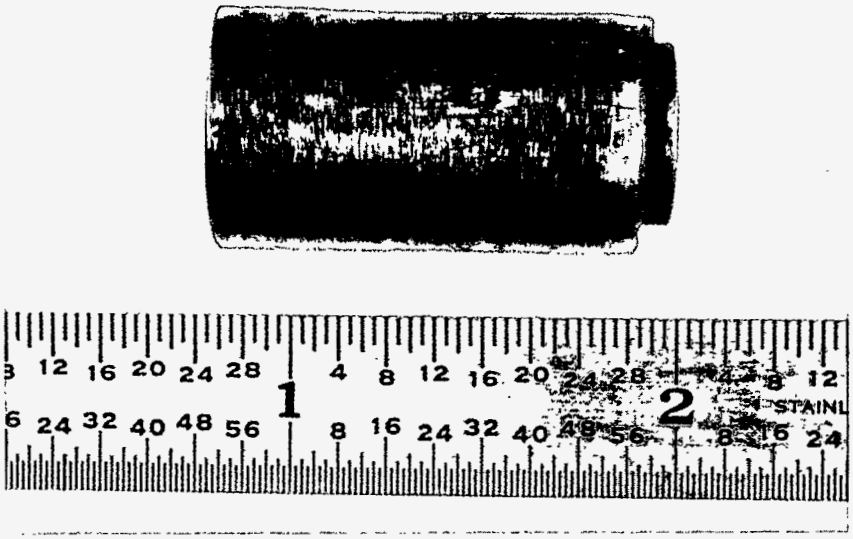

69463

a)

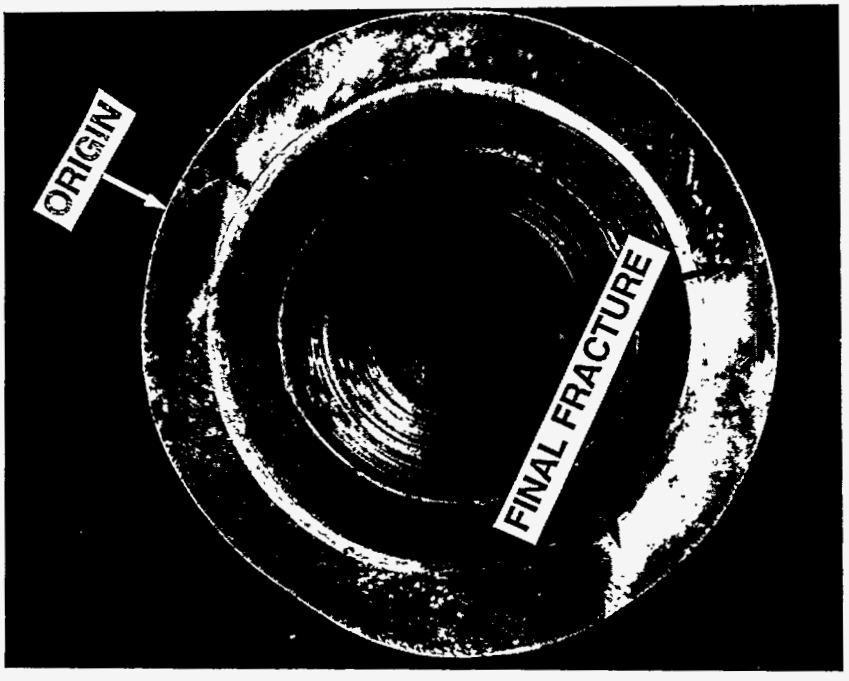

69599 3.7X

b)

FIGURE 6-2. PHOTOGRAPHS OF THE FRACTURED SURFACE TOWARDS THE GAUGE. Arrow shows discolored region.

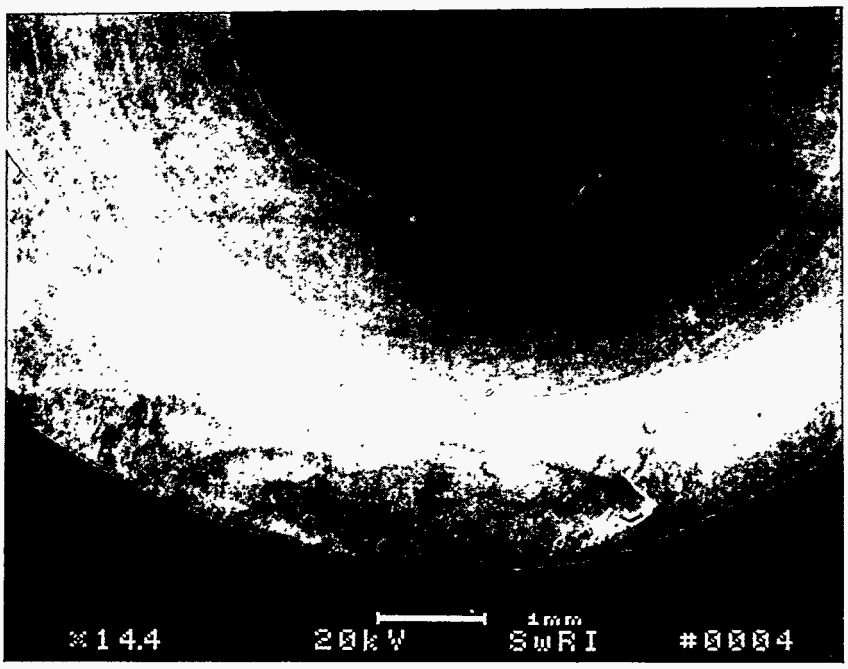

69418 14.4X

a)

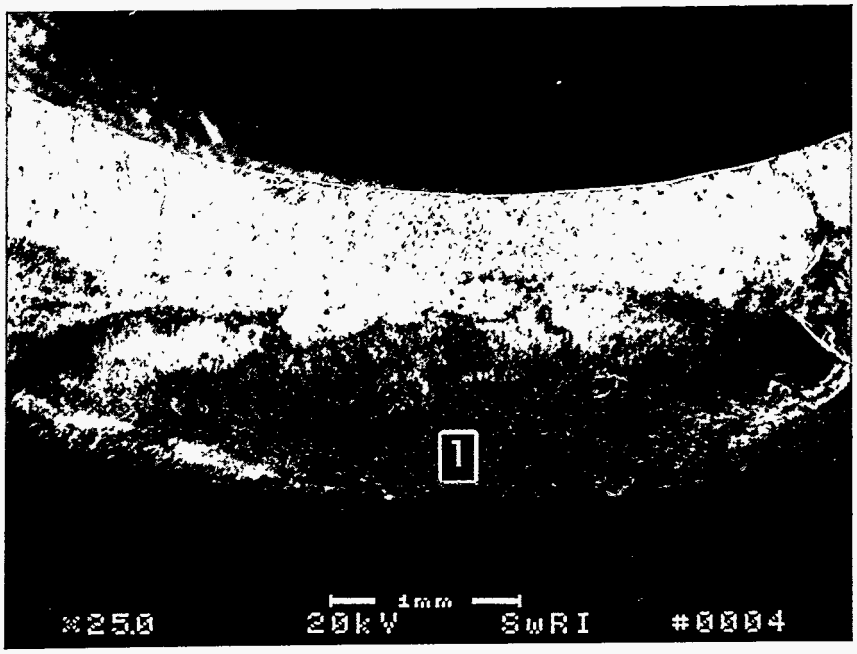

69419 25X

b)

FIGURE 6-3. SEM FRACTOGRAPHS OF THE TIP END SHOWING ELLIPTICAL REGION.

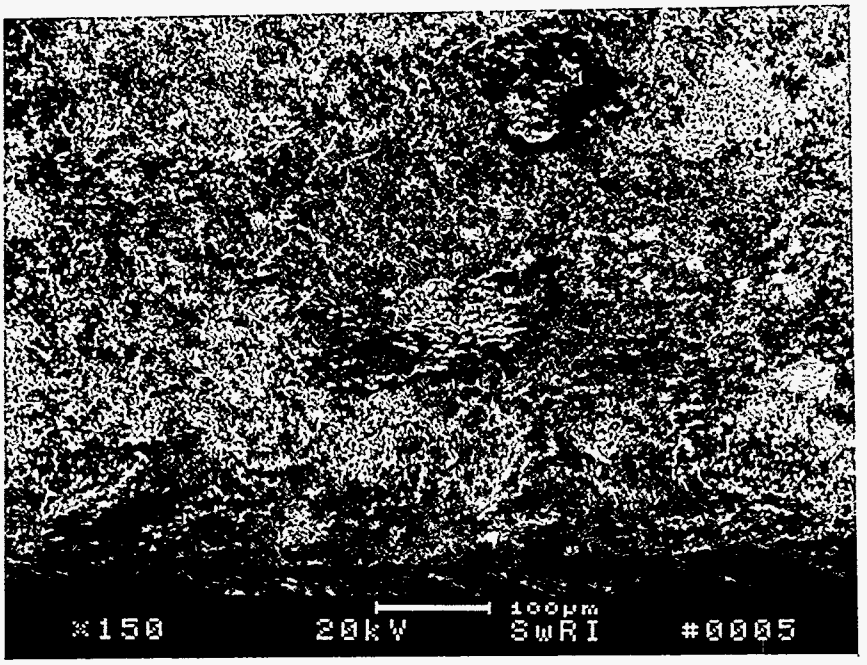

69424 150X

c) Location No. 1

FIGURE 6-3 (continued). SEM FRACTOGRAPHS OF THE TIP END SHOWING ELLIPTICAL REGION.

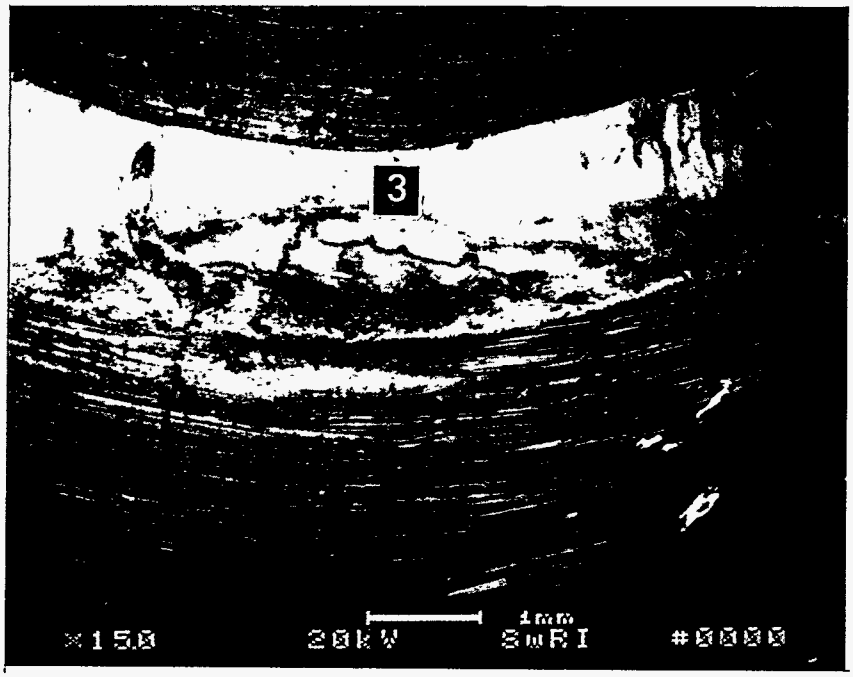

69746 15X

a)

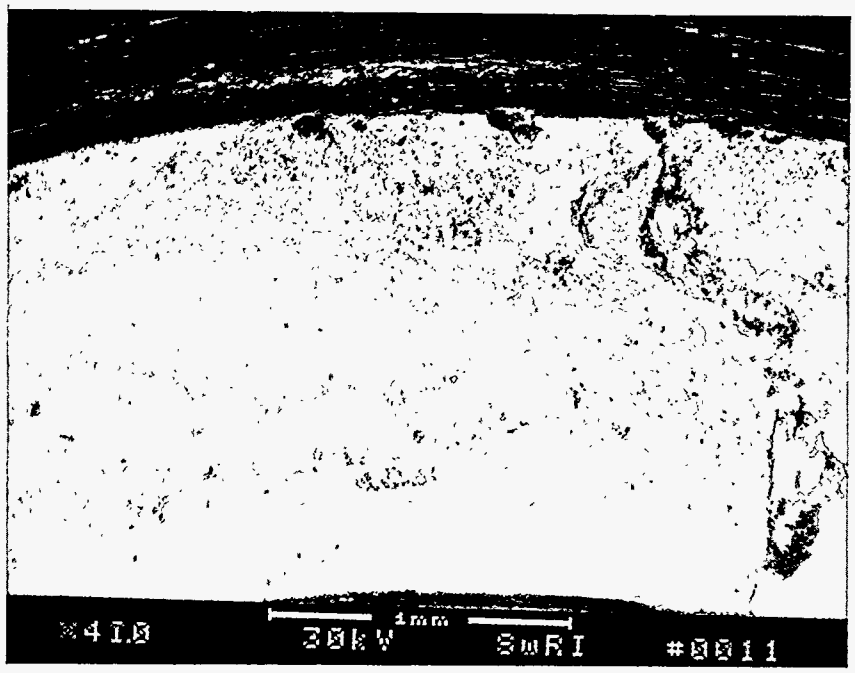

69583 41X

b)

FIGURE 6-4. SEM FRACTOGRAPHS OF ORIGIN ON GAUGE SIDE. Notice corrosion pits on the OD surface. Arrow indicates clamshell pattern.

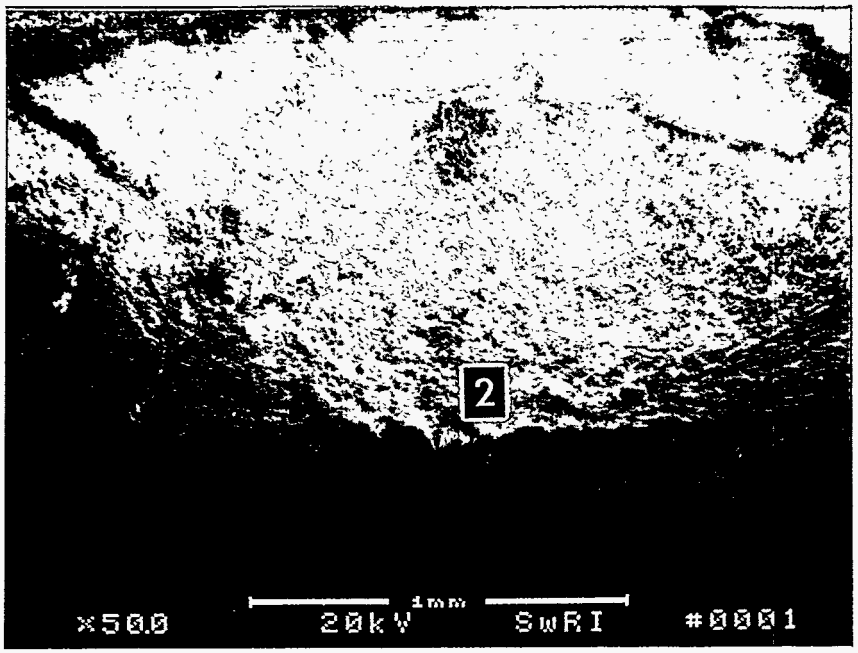

69748 50X

a)

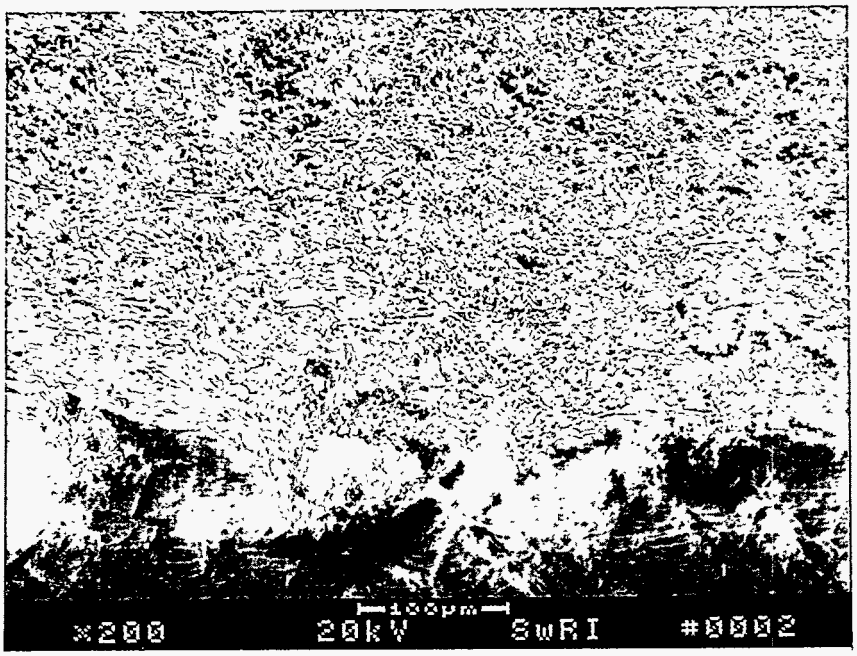

69749 200X

b)

FIGURE 6-5. SEM FRACTOGRAPHS IN THE ELLIPTICAL REGION, LOCATION 2.

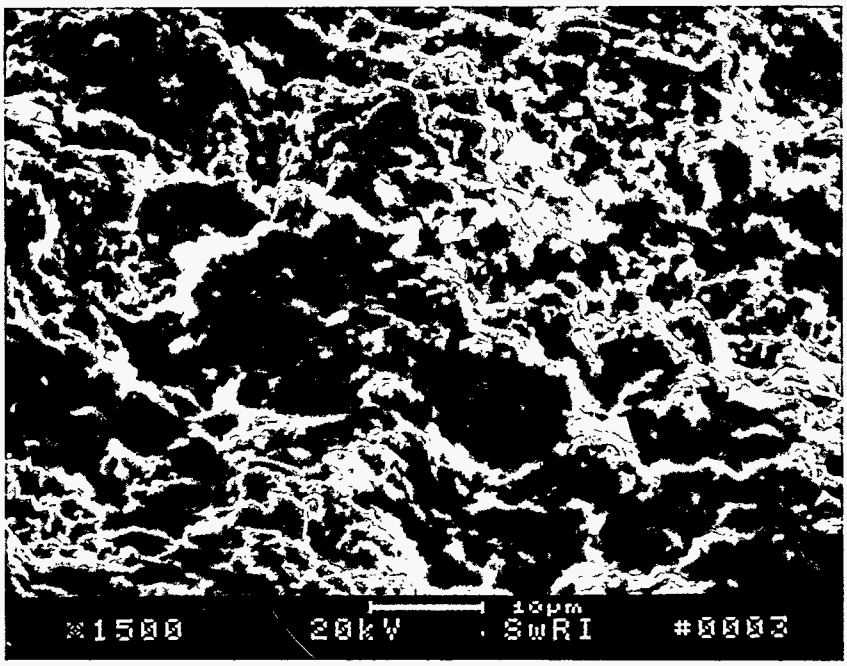

69752 1500X

c)

FIGURE 6-5 (continued). SEM FRACTOGRAPHS IN THE ELLIPTICAL REGION, LOCATION 2.

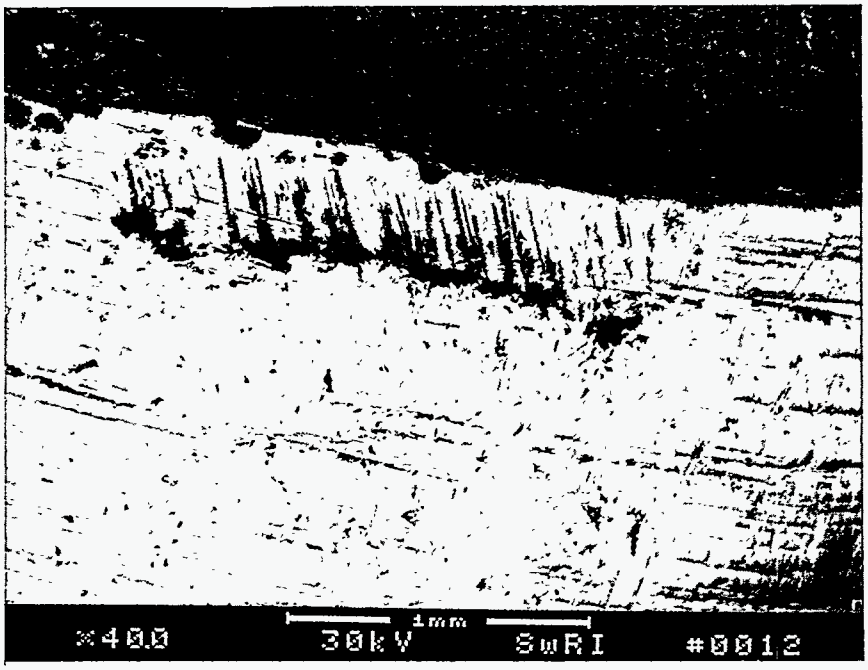

69584 40X

a)

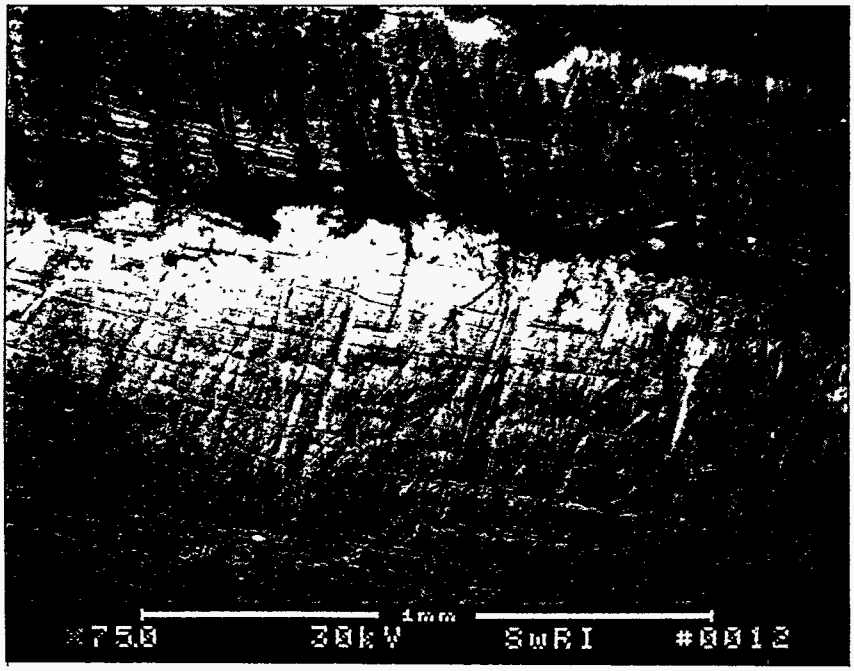

69585 75X

b)

FIGURE 6-6. SEM PHOTOGRAPHS OF ABRASIVE SCRATCH ON THE SURFACE.

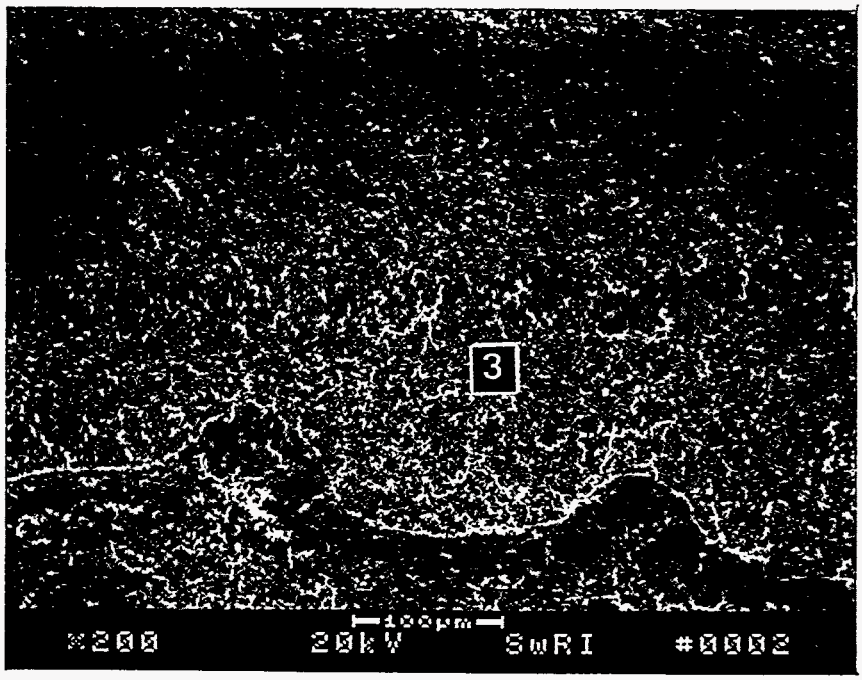

69750 200X

a)

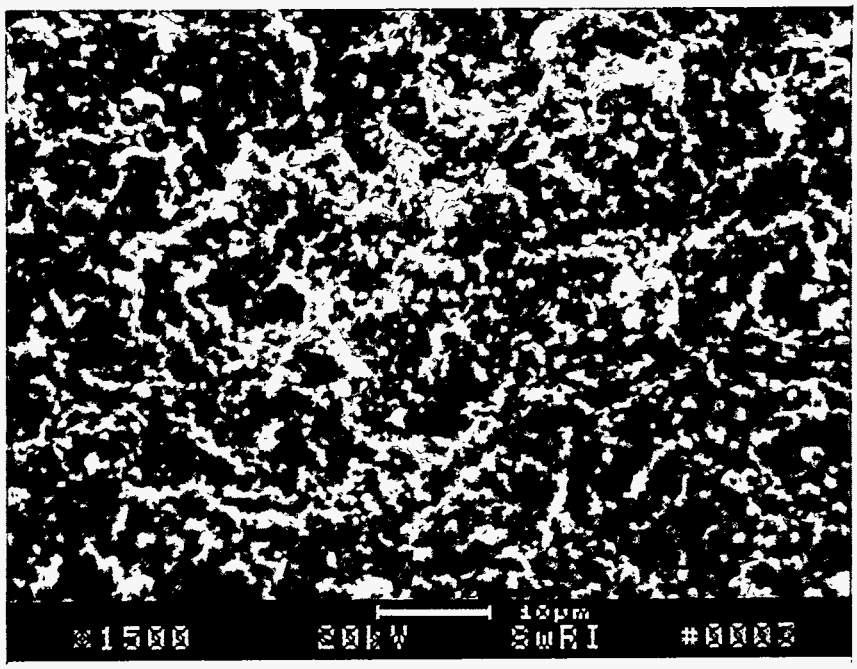

69751 1500X

b)

FIGURE 6-7. SEM FRACTOGRAPHS OUTSIDE OF THE ELLIPTICAL REGION, LOCATION 3.

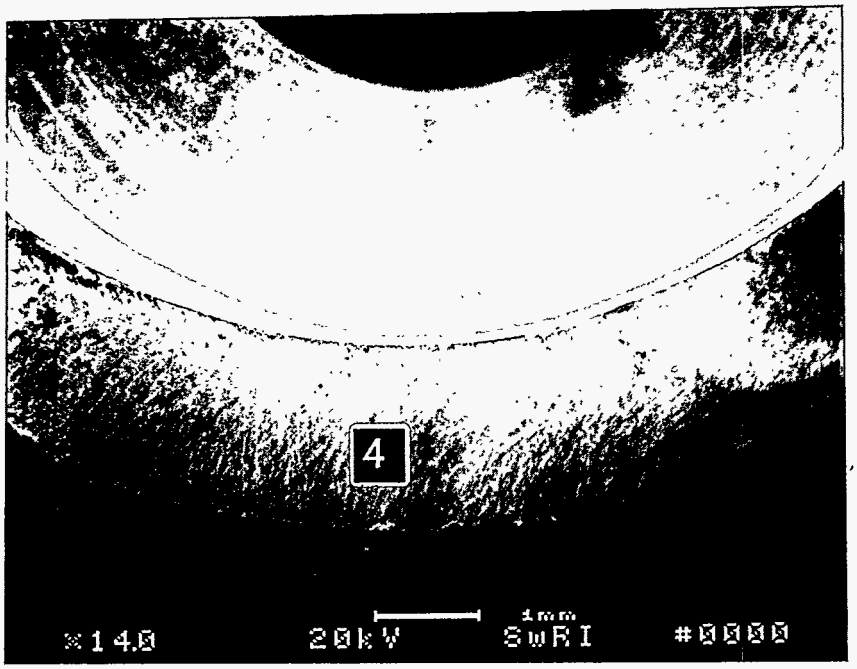

69416 14X

a)

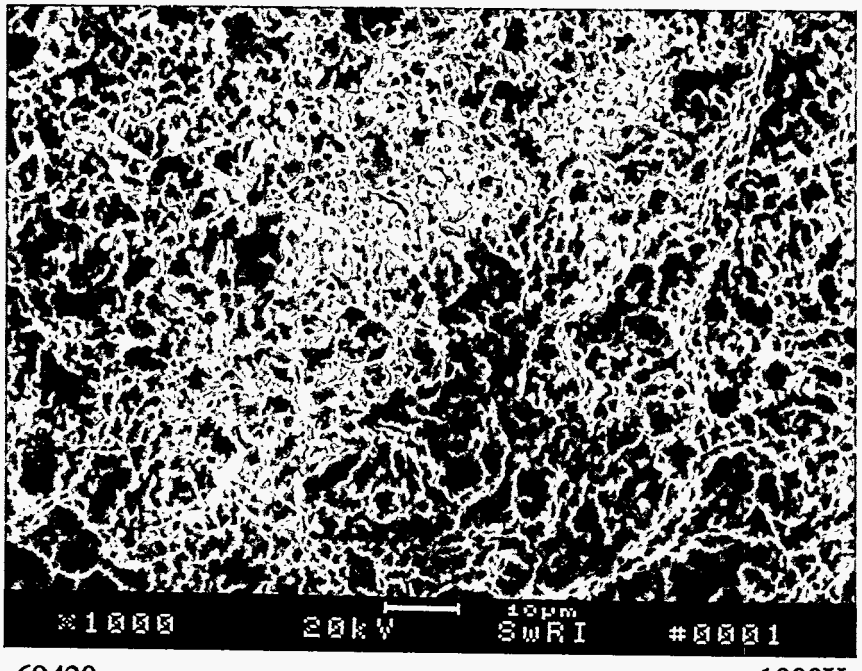

69420 1000X

b)

FIGURE 6-8. SEM FRACTOGRAPHS OF FINAL FRACTURE REGION AND LOCATION NO. 4.

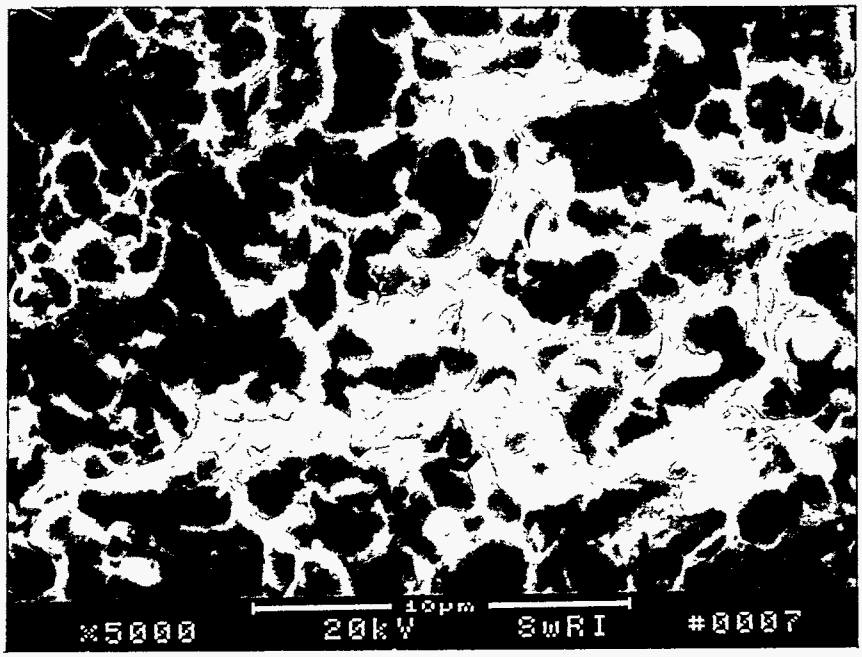

69428 5000X

c)

FIGURE 6-8 (continued). SEM FRACTOGRAPHS OF FINAL FRACTURE REGION AND LOCATION NO. 4.

7.0 Energy Dispersive X-Ray Spectroscopy

A semi-quantitative analysis was performed on Gauge No. 12711 rod, cup, weld metal, and corrosion product using Energy Dispersive X-ray (EDS) spectroscopy. The semi-quantitative analysis is not exact, but avoids destroying material. A beryllium window analysis was conducted which identifies elements as low as sodium (Na) that are present on the surface and below the surface. Table 7-1 shows the EDS results for the rod, cup, weld, and corrosion pits. The EDS spectra for each location is shown in Figures 7-1 through 7-5. The EDS determined that the rod and cup material on each side of the weld was the same. Although there was a slight discrepancy in actual weight percent, the elements and percent were in general agreement.

However, the weld metal was not the same metal as the rod. The weld metal was comparable to an austenitic stainless grade (probably Type 308).

The corrosion product analysis identified elements of calcium, chlorine, and potassium. These elements are typical for the application of the rod.

Table 7-1. EDS Results for Rod, Weld, and Corrosion Product

Sample Identification	Composition (% by weight)									
	Fe	Mn	Si	Ni	Cr	Al	S	Ca	Cl	K
Rod (Towards Housing)	78.67-	-	0.69	-	19.41	0.91	0.32	-	-	-
Rod (Towards Tip)	80.57	-	0.36	-	18.09	0.63	0.35	-	-	-
Cup	75.7	-	1.04	-	22.42	0.21	0.64	-	-	-
Weld	72.8	1.3	0.7	6.22	18.99	-	-	-	-	-
Corrosion Pit	76.21	-	6.42	-	9.74	2.25	1.76	1.51	1.11	0.99
AISI 308	Bal	1.00-2.50	0.03 Max	9.00-11.00	19.50-22.00	-	0.03 Max	-	-	-
AISI 440C	Bal	4.00 Max	0.33 Max	0.75 Max	16.0-18.0	-	0.030 Max	-	-	-

Series II Southwest Research Institute MON 10-OCT-94 15:04
Cursor: 0.000keV = 0

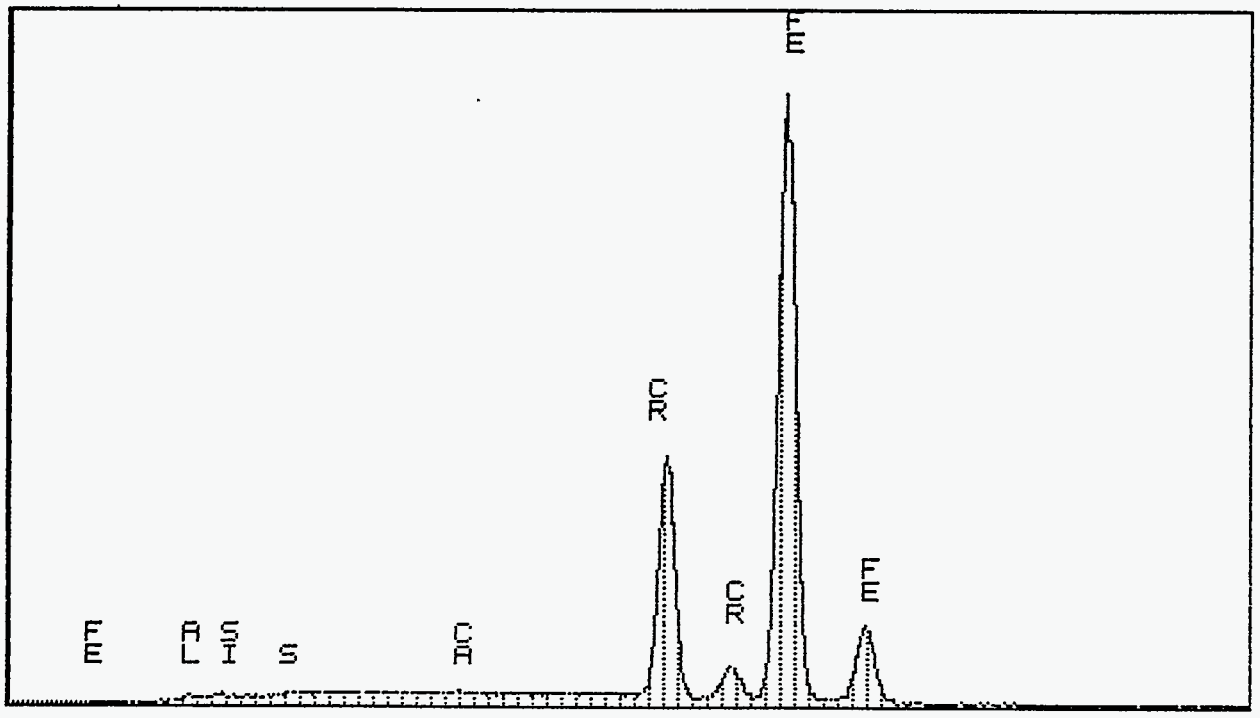

0.000 VFS = 4096 10.240

83 04-4448-011 TROXLER #12711 LOC C 30KV WD26

SQ: QUANTIFY

04-4448-011 TROXLER #12711 LOC C 30KV WD26
Standardless Analysis
30.0 KV 40.5 Degrees

Chi-sqd = 1.37

Element	Rel. K-ratio	Net Counts
Fe-K	0.75706 +/- 0.00518	68596 +/- 469
Cr-K	0.23573 +/- 0.00277	26546 +/- 312
Si-K	0.00272 +/- 0.00088	405 +/- 131
Al-K	0.00249 +/- 0.00087	313 +/- 109
S -K	0.00201 +/- 0.00091	304 +/- 137

ZAF Correction 30.00 kV 40.48 deg
No.of Iterations = 3

Element	K-ratio	Z	A	F	Atom%	Wt%
Fe-K	0.734	1.000	1.072	1.000	76.13	78.67
Cr-K	0.228	1.007	1.019	0.829	20.18	19.41
Si-K	0.003	0.918	2.863	0.998	1.33	0.69
Al-K	0.002	0.947	3.994	0.999	1.82	0.91
S -K	0.002	0.922	1.776	0.994	0.53	0.32
					Total=	100.00%

FIGURE 7-1. ENERGY DISPERSIVE X-RAY SPECTRA FOR ROD TOWARDS HOUSING.

Series II Southwest Research Institute MON 10-OCT-94 14:56
Cursor: 0.000keV = 0

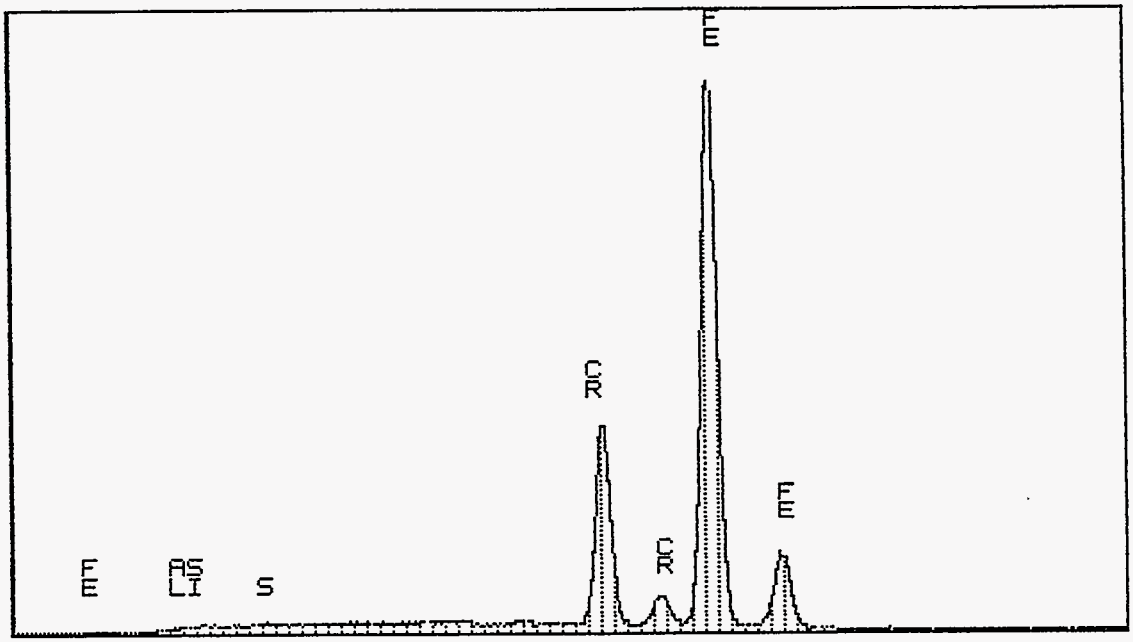

0.000 VFS = 4096 10.240

ES 04-4448-011 TROXLER #12711 LOC A 30KV WD26

SQ: QUANTIFY

04-4448-011 TROXLER #12711 LOC A 30KV WD26
Standardless Analysis
  30.0 KV 40.5 Degrees

Chi-sqd = 1.76

Element	Rel. K-ratio	Net Counts
Fe-K	0.77456 +/- 0.00515	71976 +/- 479
Cr-K	0.22014 +/- 0.00265	25424 +/- 306
Si-K	0.00139 +/- 0.00082	212 +/- 125
Al-K	0.00170 +/- 0.00081	220 +/- 104
S -K	0.00221 +/- 0.00086	343 +/- 133

ZAF Correction 30.00 kV 40.48 deg
No.of Iterations = 1

Element	K-ratio	Z	A	F	Atom%	Wt%
Fe-K	0.755	1.000	1.067	1.000	78.51	80.57
Cr-K	0.215	1.007	1.019	0.822	18.93	18.09
Si-K	0.001	0.918	2.872	0.998	0.69	0.36
Al-K	0.002	0.947	4.023	0.999	1.27	0.63
S -K	0.002	0.921	1.774	0.994	0.59	0.35
					Total=	100.00

FIGURE 7-2. ENERGY DISPERSIVE X-RAY SPECTRA FOR FLATTENED REGION NEAR TIP.

Series II Southwest Research Institute MON 10-OCT-94 14:59
Cursor: 0.000KeV = 0

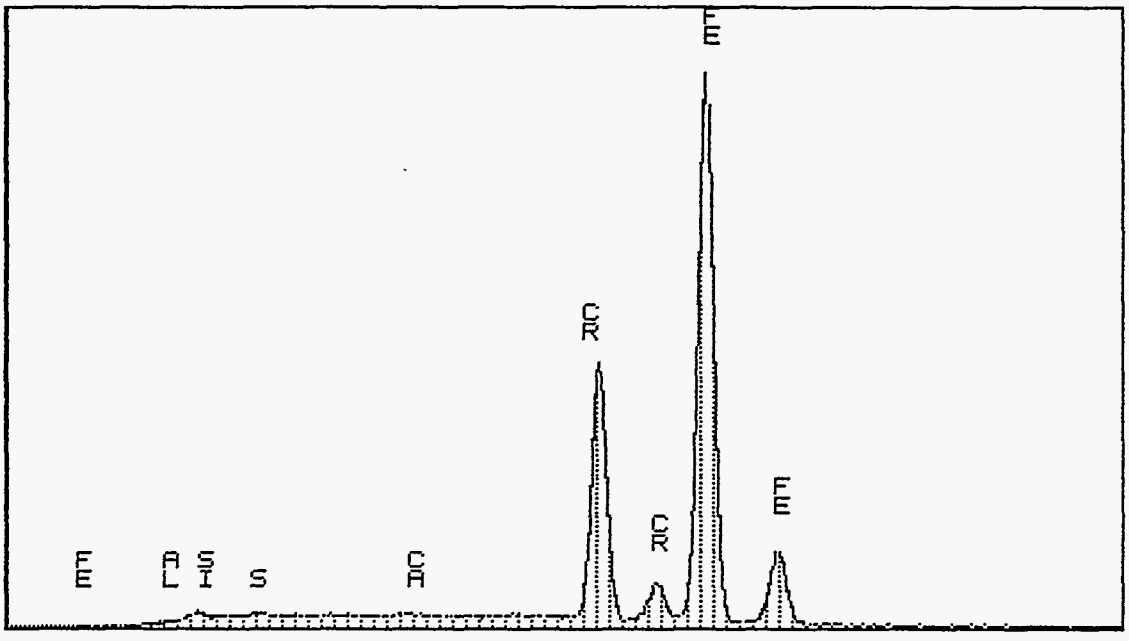

SQ: QUANTIFY

04-4448-011 TROXLER #12711 LOC D 30KV WD26
Standardless Analysis
30.0 KV 40.5 Degrees

Chi-sqd = 1.77

Element	Rel. K-ratio	Net Counts
Fe-K	0.72251 +/- 0.00493	69925 +/- 477
Cr-K	0.26869 +/- 0.00283	32319 +/- 340
Si-K	0.00416 +/- 0.00092	663 +/- 146
Al-K	0.00057 +/- 0.00089	77 +/- 119
S -K	0.00407 +/- 0.00093	658 +/- 151

ZAF Correction 30.00 kV 40.48 deg
No.of Iterations = 3

Element	K-ratio	Z	A	F	Atom%	Wt%
Fe-K	0.699	1.000	1.083	1.000	73.22	75.70
Cr-K	0.260	1.007	1.018	0.841	23.29	22.42
Si-K	0.004	0.918	2.824	0.998	2.00	1.04
Al-K	0.001	0.947	3.969	0.999	0.41	0.21
S -K	0.004	0.922	1.767	0.994	1.07	0.64
					Total=	100.00%

FIGURE 7-3. ENERGY DISPERSIVE X-RAY SPECTRA FOR CUP IN ROD.

Series II Southwest Research Institute THU 17-NOV-94 16:56
Cursor: 0.000keV = 0

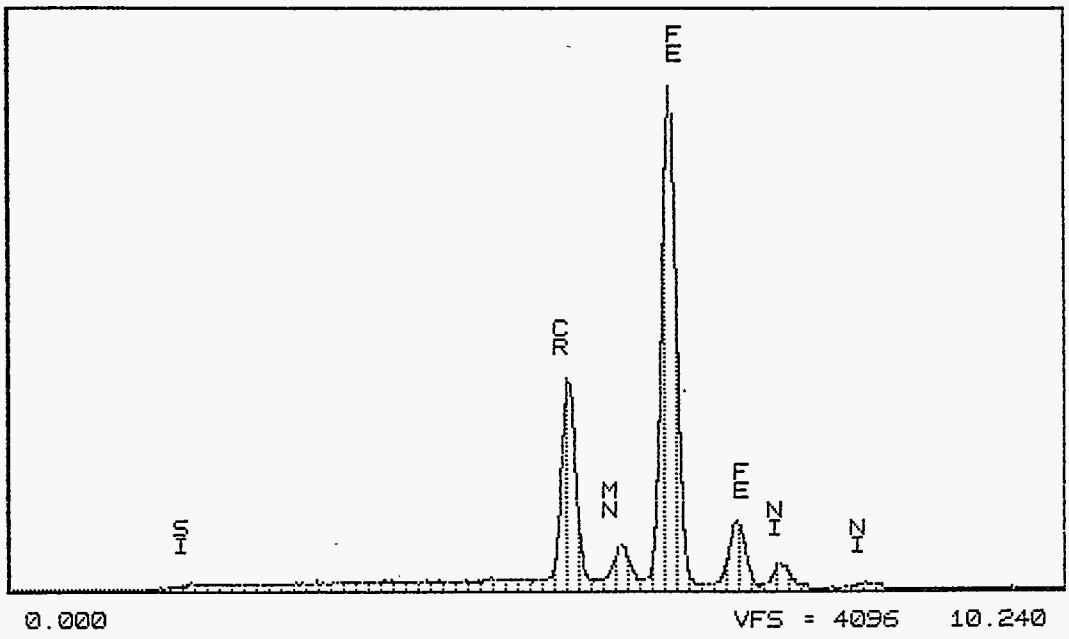

101 TROXLER, #12711, WELD MTL. - 30KV, 12MM

SQ: QUANTIFY

TROXLER, #12711, WELD MTL. - 30KV, 12MM
Standardless Analysis
30.0 KV 31.6 Degrees

Chi-sqd = 1.23

Element	Rel. K-ratio	Net Counts
Fe-K	0.70550 +/- 0.00504	66791 +/- 477
Cr-K	0.22838 +/- 0.00288	26772 +/- 338
Ni-K	0.05045 +/- 0.00258	3715 +/- 190
Mn-K	0.01324 +/- 0.00239	1402 +/- 253
Si-K	0.00243 +/- 0.00053	360 +/- 79

ZAF Correction 30.00 kV 31.62 deg
No.of Iterations = 1

Element	K-ratio	Z	A	F	Atom%	Wt%
Fe-K	0.675	1.001	1.086	0.992	71.50	72.80
Cr-K	0.219	1.007	1.024	0.842	20.03	18.99
Ni-K	0.048	0.979	1.315	1.000	5.81	6.22
Mn-K	0.013	1.023	1.008	0.993	1.30	1.30
Si-K	0.002	0.919	3.287	0.998	1.37	0.70
					Total=	100.00%

FIGURE 7-4. ENERGY DISPERSIVE X-RAY SPECTRA FOR THE WELD.

Series II Southwest Research Institute MON 10-OCT-94 14:30
Cursor: 0.000KeV = 0

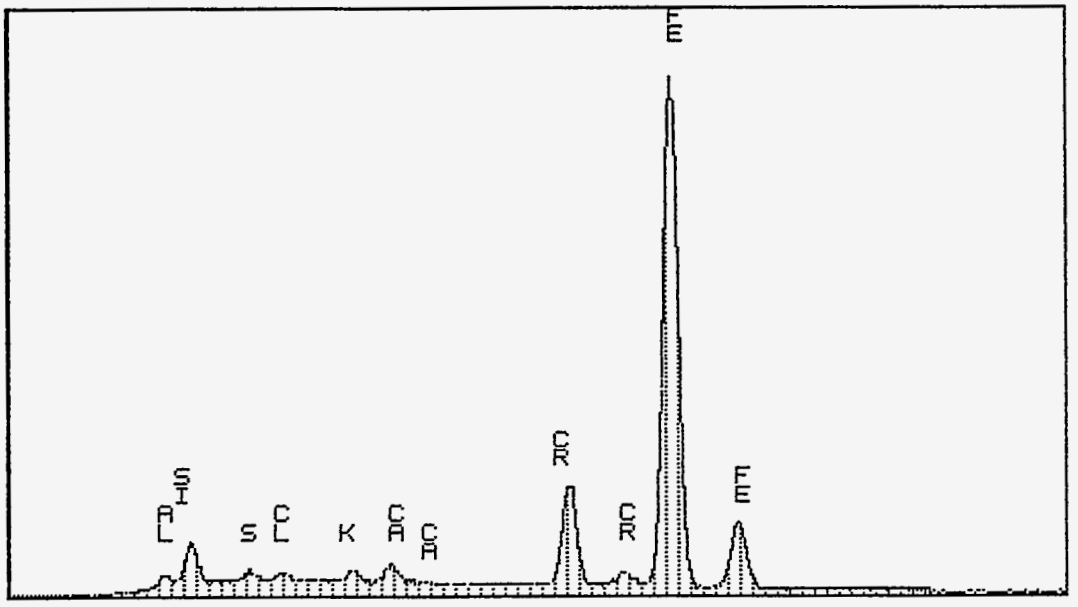

0.000 VFS = 4096 10.240

87 04-4448-011 TROXLER #12711 LOC E 30KV WD26

SQ: SETUP DEFINITIONS

SQ: QUANTIFY

04-4448-011 TROXLER #12711 LOC E 30KV WD26
Standardless Analysis
30.0 KV 40.5 Degrees

Chi-sqd = 1.07

Element	Rel. K-ratio	Net Counts
Fe-K	0.79589 +/- 0.00544	69787 +/- 477
Cr-K	0.12420 +/- 0.00240	13535 +/- 262
Ca-K	0.01593 +/- 0.00140	2316 +/- 204
K -K	0.00930 +/- 0.00119	1406 +/- 180
Cl-K	0.00814 +/- 0.00119	1253 +/- 184
S -K	0.01154 +/- 0.00136	1688 +/- 199
Si-K	0.02798 +/- 0.00145	4042 +/- 210
Al-K	0.00702 +/- 0.00133	855 +/- 162

ZAF Correction 30.00 kV 40.48 deg
No.of Iterations = 4

Element	K-ratio	Z	A	F	Atom%	Wt%
Fe-K	0.720	1.012	1.047	1.000	67.78	76.21
Cr-K	0.112	1.018	1.037	0.821	9.30	9.74
Ca-K	0.014	0.932	1.174	0.954	1.87	1.51
K -K	0.008	0.961	1.268	0.971	1.26	0.99
Cl-K	0.007	0.971	1.574	0.989	1.56	1.11
S -K	0.010	0.931	1.826	0.993	2.73	1.76
Si-K	0.025	0.927	2.742	0.997	11.35	6.42
Al-K	0.006	0.956	3.722	0.997	4.15	2.25
					Total=	100.00%

FIGURE 7-5. ENERGY DISPERSIVE X-RAY SPECTRA FOR THE ROD CORROSION.

8.0 Welding Evaluation

Metallographic examinations in this report were compared to information received from the manufacturer to better understand how the source rod-to-cup weld joints were made.

Welding Procedure

Discussions with the manufacturer of the Model 3401 gauges provided the following manufacturing/welding information.[1]

The following progression of materials were used to manufacture the source rods and source cups over the last twenty years. Choice of rod materials was determined by wear testing in which it was found that the 17-4 PH material did not provide high enough hardness based on achieving HRC 43-44 values.

Material Combinations	Source Rod	Source Cup
Initial materials	440C	440C
2nd Iteration	17-4PH	17-4PH
3rd Iteration	17-4PH	440C

Heat Treatment The source cup and rod parts were hardened before welding.

Welding Process The gas tungsten arc welding (GTAW) process was used.

Filler Material Type ER 308 stainless steel filler metal was used

Joint Configuration The source rod was counter bored to provide a wall thickness of 0.075 inch, then partially chamfered to provide a single bevel weld preparation. The source cup was counter bored and machined to provide integral backing of similar wall thickness to fit closely into the source rod counter bore.

[1] John Egan, Troxler engineer discussed the following welding parameters by telephone with Mr. Schick of Southwest Research Institute on March 21, 1994.

Welding Procedure	A fixture was used to provide shielding during welding. No preheat was used. Good welding process control was maintained by operator training. Welds were ground after welding.
Certification	No specific welding standard was used to certify welding, however, the procedure was controlled by Troxler manufacturing practice.
Quality Control	Visual inspection was performed on all welds. Liquid penetrant inspection is also presently performed on finished rods.

Welding Assessment

The metallurgical examination of the weld confirmed the information provided by Troxler with the following observations.

Joint Configuration	One side of the joint was reported to be ground to provide a bevel groove and possibly with a relief groove to allow filler metal to penetrate without consuming the integral backing (Refer to Figure 5-1). Alignment of this groove did not coincide with the root of the weld, however no welding flaws occurred as a result. Note that the welding heat and width of weld extends considerably toward the cup side of the joint. Directing the arc to the cup side is evidently necessary to promote fusion with the heavier section. Refer to the photomacrographs of Gauge No. 12711 shown in Figure 5-2.
Heat Treatment	Because the source cup and rod parts were hardened before welding, a sharp microstructural transition was produced by the weld as indicated by the heat affected zone shown in Figure 5-2.
Weld Root	Inadequate penetration of the weld root also is shown in Figure 5-2, was probably caused by misalignment of the joint over the backing groove.

Examinations of the weld and joint indicate that only one side of the joint had a bevel groove which resulted in high heat input on the side that had the high hardness zone. The hardened zone and microstructure indicate that no post weld treatment was performed on the weld. See Section 9.0 for more discussion.

9.0 Discussion

The following observations were made during investigation of the Troxler gauges.

1) Gauge No. 12711 failed in a brittle manner. Fractographic features indicated that cracking initiated on one side.

2) The origin region on the one side consisted of discolored region, pitting, and abrasive marks.

3) Fractographic features in the discolored region consisted of a heavily oxidized fracture surface and crack arrest bands. These features indicate that a small crack had existed for some time. The surface corroded, then during usage the crack extended, then arrested until the next usage.

4) The fracture surface outside of the discolored region was slightly oxidized as the crack extended around the circumference. The final fracture region was not oxidized. This indicates that a large crack was present before catastrophic fracture occurred.

5) Hardness tests determined that in the region of crack initiation, the material was very hard (HRC 62), but the weld was very soft (HRC 21).

6) Hardness tests on the other four rods determined the welds were soft indicating that the other rods were welded in the same manner as the failed rod.

7) The source rod and cup alloy was 440C which is a hardenable chrome steel. The rod and cup were welded using an austenitic stainless steel, likely AISI 308.

8) The alloy of the other rods could not be definitely confirmed unless chemical analysis tests are performed. However, the hardnesses were comparable to the 440C alloy.

SwRI concludes that the rod failed in a brittle manner indicated by the flat surface features and the lack of deformation. The brittle fracture occurred because of a hard zone that resulted from welding the rod. Type 440C is a difficult alloy to weld. Consequently, the combined effects of the joint configuration and welding procedure resulted in the hard zone. From the fractographic and surface features, it appears that the rod was in a severe bending condition. The high bending condition in conjunction with a hard zone resulted in initiation of a small crack.

Fractographic features indicate that although the fracture was characteristic of a brittle failure, the crack had progressively extended during multiple uses. In other words, the rod did not fail catastrophically due to a one time load. It failed progressively over time due to multiple loadings. The arrest marks are indicative of a crack stopping, then extending under multiple loads. In addition, most of the fracture surface was transgranular and flat in appearance. A sudden load failure in a brittle material will often have cleavage facets. Only the final fracture had evidence of cleavage facets. Because the crack propagation was progressive with evidence of slow crack growth, if 440C rods are subjected to similar conditions as Gauge Nos. 12711 and 12712, then cracking is probable. A routine visual and dye-penetrant inspection should detect any rods that are cracked. SwRI believes not all rods are cracked or will crack. However, rods subjected to high bending conditions are prone to crack.

Fractographic features indicated that crack initiation occurred on one side. However, the exact cause for initiation is inconclusive. There does appear to be many contributors for a crack to initiate. The microstructural analysis and hardness evaluation indicated that at the location of the origin, the material was the hardest (HRC 61). Although the rod did not fail directly because of high hardness, the high hardness made the rod more susceptible to crack initiation if a stress concentration existed with a high load.

A stress concentration was present because of two factors. First, the large differential in hardness between the HAZ and the weld metal caused a microstructural stress concentrator. Second, the superficial pitting was found on the surface and was evident at the origin. Corrosion of Type 440C is not unusual. Although pitting was present, it is believed that the pits alone were not a cause for failure. The reason is because pits were evident at other locations, but no cracks were found extending from the pits.

For the rod to crack, there needed to be a high load condition. There is a possible explanation for a high load condition; e.g., if the user did not follow the instructions and forced the rod into the ground or asphalt. If that is the case, then stresses would concentrate at the weld. The fact that the origin was on one side and the fact that an abrasive mark was present in the vicinity of the origin, suggests an impact occurred. Consequently, the rod was in a bending condition at the high hardness region. The other side did not have evidence of a crack caused by bending.

The material used, Type 440C, is generally a difficult alloy to weld. Usually close controls are needed on preheat and postheat conditions. It would appear that the rod was welded with a Type 308 welding rod to minimize welding problems. Based on the high hardness values, it appeared that the rod was not postweld heat treated. In the case of Type 440C, there are several concerns: 1) a high hardness indicates that the rod had low ductility, 2) the large differential in the hardness between the base metal and weld causes a microstructural stress concentration, 3) the 440C in the welded condition has lower impact properties. The impact properties are even lower at lower usage temperatures. For these reasons, SwRI believes the welded condition of the Type 440C was not the optimum for this application.

The combined factors of a poor weldability of Type 440C, the joint configuration, and the lack of a post weld heat treatment explains the high hardness zone. The alloy Type 440C is considered to have very low weldability because of the carbon content or carbon equivalent

(CE) which makes it highly hardenable and susceptible to cold cracking during welding and is seldom considered for applications involving welding. Welding produces a hardened martensitic zone adjacent to the weld. The hardness of the HAZ depends primarily on the carbon content of a base metal. As hardness increases, toughness decreases, and the zone becomes more susceptible to cracking. Alloys containing carbon equivalent content values of 0.30% or more are considered to be non-weldable without taking special precautions. These precautions generally include preheating, interpass temperature control, and post weld heat treatment requirements. Welding without these precautions is not recommended and an alternative choice of alloy or manufacturing/welding procedure controls should be recommended.

The weld joint configuration used for the rods promotes overwelding, producing a much larger weld deposit than necessary. The amount of filler metal and welding required could be reduced by preparing both parts to be joined with 30 degree bevels to give a 60 degree included angle vee groove. A nominal 1/32" root gap would give adequate penetration and reduce the welding heat required. The counter bore on the cup side of the joint, with the integral backing, could be increased to remove the heavy wall thickness from the proximity of the weld. This would promote fusion with both sides of the joint so that the welding heat need not be directed more to one side.

An improved welding procedure could reduce the high hardness. The heat treatment recommended should be included with the welding procedure requirements for the purpose of reducing the hard brittle transition of the HAZ. A minimum of 500°F preheat is recommended for carbon contents over 0.50% before welding. Maintaining this preheat as a minimum interpass temperature through to post weld heat treat is recommended by tempering immediately after welding without cooling to room temperature. Typical tempering for this alloy for stress relieving is done from 300 to 800°F. Post weld heat treatment in the form of a localized stress relief might soften this zone. Using the temper bead technique to deposit the cover-pass weld beads also might produce sufficient softening of the HAZ to minimize the "brittle notch" condition.

SwRI understands that Troxler's present practice now provides for a threaded source rod-to-cup connection with a seal weld joint design. This will eliminate the possibility of losing the source cup in the future.

NRC FORM 335 (2-89) NRCM 1102, 3201, 3202

U.S. NUCLEAR REGULATORY COMMISSION

BIBLIOGRAPHIC DATA SHEET

(See instructions on the reverse)

1. REPORT NUMBER (Assigned by NRC, Add Vol., Supp., Rev., and Addendum Numbers, if any.)
NUREG/CR-6074
04-4448-010
Vol. 5

2. TITLE AND SUBTITLE
Sealed Source and Device Design Safety Testing
Technical Report on the Findings of Task 4
Investigation of Failed Radioactive Stainless Steel Troxler Guages

3. DATE REPORT PUBLISHED
MONTH: October | YEAR: 1995

4. FIN OR GRANT NUMBER
D2553

5. AUTHOR(S)
D.J. Benac, W.R. Schick

6. TYPE OF REPORT

7. PERIOD COVERED *(Inclusive Dates)*

8. PERFORMING ORGANIZATION – NAME AND ADDRESS *(If NRC, provide Division, Office or Region, U.S. Nuclear Regulatory Commission, and mailing address; if contractor, provide name and mailing address.)*
Southwest Research Institute
6220 Culebra Road
San Antonio, TX 78238-5166

9. SPONSORING ORGANIZATION – NAME AND ADDRESS *(If NRC, type "Same as above"; if contractor, provide NRC Division, Office or Region, U.S. Nuclear Regulatory Commission, and mailing address.)*
Division of Industrial and Medical Nuclear Safety
Office of Nuclear Material Safety and Safeguards
U.S. Nuclear Regulatory Commission
Washington, DC 20555-0001

10. SUPPLEMENTARY NOTES

11. ABSTRACT *(200 words or less)*

This report covers the Task 4 activities for the Sealed Source and Device Safety testing program. SwRI was contracted to investigate failed radioactive stainless steel troxler gauges. SwRI's task was to determine the cause of failure of the rods and the extent of the problem. SwRI concluded that the broken rod failed in a brittle manner due to a hard zone in the heat affected zone.

12. KEY WORDS/DESCRIPTORS *(List words or phrases that will assist researchers in locating the report.)*
sealed source, safety testing, failed guages

13. AVAILABILITY STATEMENT
unlimited

14. SECURITY CLASSIFICATION
(This Page)
unclassified
(This Report)
unclassified

15. NUMBER OF PAGES

16. PRICE